Environmental Health Perspectives
Vol. 64, pp. 283-295, 1985

Free Radicals of Benzo(a)pyrene and Derivatives

by Paul D. Sullivan*

The evidence for biological involvement, the spectroscopic properties (especially EPR), and the reactions, of free radicals derived from benzo(a)pyrene and its methylated, hydroxylated, and fluorinated derivatives are reviewed.

Introduction

There is a continuing interest in the possibility that free radicals are involved as intermediates in the metabolism of polycyclic hydrocarbons in general and of benzo(a)pyrene in particular. Free radicals may be derived directly from benzo(a)pyrene (BaP) under a variety of conditions. At least four different radicals have been characterized to various degrees by electron paramagnetic resonance (EPR) spectroscopy. The simplest radical species are formed by either a one-electron reduction to give the anion radical ($BaP^{\cdot-}$) (*1*) or a one-electron oxidation to give the cation radical ($BaP^{\cdot+}$) (*2–5*). Another radical species is formed from BaP when it is heated above the melting point (*6*), the EPR analysis is consistent with a rearranged product, but has not been unequivocally identified. Oxygenated radicals can be produced from BaP under various reaction conditions. The most prominent oxygenated radical has been identified by several groups as the 6-oxybenzo(a)pyrene radical (*3,7–12*). Other oxygenated radicals may be generated from the 1,6-, 3,6-, and 6,12-BaP-diones (*3,13*).

Evidence for Biological Involvement of BaP Radicals

BaP Cation Radical

This radical was first hypothesized as a reactive metabolic intermediate of BaP by Wilk et al. (*14*) and Fried and Schumm (*15*). Since these first reports, much circumstantial evidence has been presented for the biological involvement of BaP cation radicals. Unfortunately, the reactivity of the BaP cation radical has precluded its direct observation in either *in vivo* or *in vitro* systems, it has only been directly observed in model systems. Much of the early evidence was based upon the fact that BaP has a sufficiently low oxidation potential that it can be oxidized chemically by weak oxidants such as I_2 or $FeCl_3$ to give radical species which can be observed by EPR or trapped by various nucleophiles (*10,16–18*). Since I_2 and other Fe(III) compounds have been shown to oxidize other polycyclic hydrocarbons to their respective cation radicals (*19-20*) it is hypothesized that, *in vivo*, BaP could be oxidized by a one-electron transfer to cytochrome-P-450 [Eq. (1)].

$$\text{BaP} + \text{Fe(III)-Cyt-P-450} \rightleftarrows \text{BaP}^{\cdot+} + \text{Fe(II)-Cyt-P-450} \quad (1)$$

This reaction would presumably compete with the normal oxygen addition or insertion reactions of cytochrome P-450. The chemical reactivity of the BaP cation radical indicates that nucleophilic trapping of the cation radical occurs almost exclusively at the 6 position, which is the site of highest charge density (*17,18,21–24*). That the nucleophile could be DNA is indicated by covalent binding of BaP to DNA in the presence of iodine (*25,26*). The limited binding of BaP to DNA in the presence of Cyt-P-450, but in the absence of oxygen is taken as indirect evidence for the *in vitro* formation of $BaP^{\cdot+}$, as are studies which show loss of tritium from position 6 of BaP during binding to DNA on mouse skin (*27*). The electro-chemical oxidation studies of Jeftic and Adams (*23*) suggest that $BaP^{\cdot+}$ should react rapidly with water to produce 6-hydroxy-BaP [Eq. (2)]. However, *in vitro* experiments by Rispin et al. (*11*) indicate that the source of oxygen in 6-hydroxy-BaP is molecular oxygen, and that it must be produced by reaction of BaP with cyt-P-450 [Eq. (3)].

$$\text{BaP}^{\cdot+} + \text{H}_2\text{O} \xrightarrow{-e^-} \text{6-OH-BaP} + 2\text{H}^+ \quad (2)$$

$$\text{NADPH} + \text{H}^+ + \text{BaP} + \text{O}_2 \xrightarrow{\text{cyt-P-450}} \text{6-OH-BaP} + \text{NADP}^+ + \text{H}_2\text{O} \quad (3)$$

It would, therefore, appear that the evidence for the involvement of the BaP cation radical in the metabolism

*Department of Chemistry, Ohio University, Athens, OH 45701.

of BaP is open to interpretation, but at the maximum, it only makes a minor contribution in the case of rat liver with, perhaps, a larger contribution for mouse skin.

This situation may be somewhat different for substituted BaP's especially those with electron donating substituents which will lower the oxidation potential and hence make Eq. (1) more favorable. For example, 6-methyl-BaP is more easily oxidized to a cation radical than is BaP (*28–30*), and nucleophilic trapping occurs predominantly at the 6-methyl group, presumably via a carbonium ion intermediate [Eq. (4)] (*31,32*).

$$\text{6-CH}_3\text{-BaP} \xrightarrow{-1e^-} \text{6-CH}_3\text{-BaP}^{\ddagger} \xrightarrow[-H^+]{-1e^-} \text{6-CH}_2^{+}\text{-BaP} \xrightarrow{\text{Nuc}} \text{6-Nu-CH}_2\text{-BaP} \quad (4)$$

Whether such a reaction occurs *in vivo* might be answered by observing if the oxygen atom in the major metabolite of 6-methyl-BaP, namely 6-hydroxymethyl-BaP, is derived from water or molecular oxygen. The carbonium ion, formed either from the cation radical directly or from hydroxymethyl esters (*33,34*), could also bind to DNA, and evidence has been presented that a major *in vivo* adduct of 6-methyl-BaP is identical to a product formed on incubation of 6-methyl-BaP with horseradish peroxidase/hydrogen peroxide and DNA (*35*) and to standards produced by reactions of a 6-methyl-BaP cation radical salt or 6-bromomethyl-BaP with DNA (*36*).

Despite the lack of direct evidence for the biological involvement of BaP cation radicals it is worthwhile to investigate the EPR spectra of these species. The potential information which may be obtained regarding the electron densities in the highest occupied molecular orbital (HOMO) could be used to explain some of the metabolic products of BaP, as well as indicate the possible electronic effects of substituents on these pathways.

Oxygenated BaP Radicals

The major metabolic pathways of BaP seem to involve two mutally exclusive processes (*37,38*), both catalyzed by cytochrome P-450. The epoxidation pathway involves stereospecific or stereoselective oxygen addition across a double bond to form one of several epoxides. These epoxides may be hydrolyzed (stereospecifically by the epoxide hydrase enzyme) to dihydrodiols or may spontaneously isomerize to phenols (*39*). The formation of the BaP trans-4,5-, 7,8- and 9,10-dihydrodiols and the 3- and 9-phenols are believed to occur via this pathway. *In vivo* the diols and phenols can be further converted to water-soluble conjugates. Further stereoselective reactions of the dihydrodiols and phenols with cytochrome P-450 can lead to secondary metabolites such as diol epoxides and epoxyphenols. The most important secondary metabolite is the *anti*-7,8-diol-9,10-epoxide, which is a major ultimate carcinogenic form of BaP (*40,41*). The free-radical or one-electron oxidation pathway involves the enzymatic formation of 6-hydroxy-BaP via a direct oxygen insertion mediated by cytochrome-P-450, or possibly via the reaction of the enzymatically formed BaP cation radical with water. The 6-hydroxy-BaP is then rapidly oxidized in several one-electron steps via an intermediate radical identified as 6-oxy-BaP, (the phenoxy radical derived from 6-hydroxy-BaP), to produce a mixture of 1,6-,3,6-, and 6,12-BaP-diones (*3,8,9,11*). 6-Hydroxy-BaP is not detected as a stable metabolite of BaP, and Nagata et al. were the first to show that its presence could be detected by observation of the EPR signal of the 6-oxy-BaP radical in rat liver homogenate metabolism of BaP (*3,42*). Ts'o et al. (*8,9*) showed that the EPR signal obtained with BaP is identical to that obtained from chemical and enzymatic oxidation of 6-hydroxy-BaP. It was also shown that the 6-hydroxy-BaP was the precursor of most, if not all, of the BaP-diones (1,6-, 6,12-, and 3,6-) formed during the metabolism of BaP (*9*). Approximately 18 to 20% of metabolism in rat liver homogenates was found to proceed via this pathway. The autoxidation of 6-hydroxy-BaP appears to be mediated by molecular oxygen and may proceed in a number of general steps [Eqs. (5)–(8)].

$$\text{6-OH-BaP} + O_2 \rightarrow O_2^{\cdot-} + [\text{6-OH-BaP}]^{\ddagger} \xrightarrow{-H^+} \text{6-oxy-BaP} \quad (5)$$

$$\text{6-oxy-BaP} + H^+ + O_2 \rightarrow \text{BaP-diols (1,6-, 3,6-, 6,12-)} + O_2^{\cdot-} \quad (6)$$

$$\text{BaP-diol} + O_2 \rightleftarrows \text{BaP-semiquinone} + O_2^{\cdot-} + 2H^+ \quad (7)$$

$$\text{BaP-semiquinone} + O_2 \rightleftarrows \text{BaP-dione} + O_2^{\cdot-} \quad (8)$$

The oxygen radicals produced may react further [Eqs. (9)–(11)].

$$2O_2^{\cdot-} + 2H^+ \rightleftarrows 2HO_2\cdot \quad (9)$$

$$2HO_2\cdot \rightleftarrows H_2O_2 + O_2 \quad (10)$$

$$O_2^{\cdot-} + H_2O_2 \rightleftarrows OH\cdot + OH^- + O_2 \quad (11)$$

The appearance of H_2O_2 during the course of the autoxidation (*9*) makes it likely that the reactive superoxide and hydroxyl radicals are also produced during the course of the reaction. The toxicity of the BaP diones to cells in culture (*43*) and their ability to induce strand breakage in T7 DNA has been attributed to the cycling between the BaP-diols and BaP-diones [Eqs. (7)-(8)], via an intermediate semiquinone radical, which would produce large amounts of reactive oxygen radicals. The production of hydroxyl radicals also indicates the possibility of a positive feedback mechanism, since hydroxy radicals, generated by Fenton's reagent, have been observed to react with BaP to generate 6-oxy-BaP radicals and BaP diones (*12,44*).

It has been proposed that after a BaP molecule is

committed to either the epoxidation or free-radical pathway there is no exchange of intermediates between the pathways (*37*). It has been further suggested that the epoxide pathway is the major activation pathway and that the free radical pathway is an important detoxification pathway (*37,45,46*). However, in view of the ability of 6-hydroxy-BaP to bind to DNA, as well as its known toxicity (*43*) and mutagenicity (*47*), together with the previously noted effects of BaP-diones, it can hardly be considered a totally benign pathway.

Other BaP Radicals

No evidence for the biological involvement of the BaP anion radical has been proposed, nor for the radical produced on heating BaP, although it may be related to radicals produced in cigarette smoke (*48*).

EPR Studies

Cation Radicals from BaP and Methylated Derivatives

The EPR spectrum of the BaP cation radical in H_2SO_4 was first observed 25 years ago (*2*) and has since been investigated by several groups (*3–5*), but only recently has a complete analysis been proposed (*29,49,50*). The interpretation of the BaP cation radical EPR spectrum was made difficult due to the asymmetry of the molecule which indicates that all 12 protons should be nonequivalent, leading to a maximum possible 2^{12} (4096) lines in the EPR spectrum. Attempts to simplify the spectrum of BaP in H_2SO_4 using electron nuclear double resonance (ENDOR) were unsuccessful due to the low signal intensity of the EPR spectrum. In an effort to obtain more signal intensity the BaP cation radical was generated (*10*) with a variety of one-electron oxidizing systems, i.e., I_2, $AlCl_3$, $SbCl_5$, $FeCl_3$, BF_3, trifluoroacetic acid/trifluoroacetic anhydride, and thallium (III) tristrifluoroacetate in trifluoroacetic acid, TTFA/TFA. In none of these systems were large amounts of cation radicals generated. Only in the case of TTFA/TFA were EPR spectra of cationic species obtained in high intensity and with high resolution (*10,51*). Unfortunately, the spectra in TTFA/TFA are not identical to those produced in H_2SO_4. From previous studies on the behavior of anthracene in TTFA/TFA it was determined (*52*) that the 6-position of BaP is trifluoroacetoxylated and the EPR spectra observed are due to the 6-trifluoroacetoxy-BaP cation radical. It was therefore concluded that only in H_2SO_4 was the cation radical of BaP produced with sufficient resolution to attempt an analysis. A method to estimate and assign the splitting constants in BaP was suggested (*29*) with the availability of all 12 monomethylated BaP's. The total width of the EPR spectrum of a monomethyl-substituted BaP should be larger than the width of the BaP spectrum by twice the methyl proton splitting at the substituted position. This assumes that the three methyl proton splittings are similar in magnitude to the single proton splitting they are replacing and that the sum of the spin densities at the remaining 11 positions remains constant. In reality, some changes are to be expected due to the perturbation of the methyl group, but canceling effects may keep the errors small. The measured widths together with the estimated methyl splittings at the substituted position are shown in Table 1. Justification for the approximations made can be obtained from the EPR spectral width of several dimethyl-BaP cation radicals in H_2SO_4. One can predict the width from the monomethylated values. The experimental and predicted values, in parentheses, for dimethyl BaP cation radicals are: 4,5-, 33.8 (34.5); 1,2-, 35.1 (34.85); 1,4-, 36.2 (35.65); 2.3-, >34.0 (36.8); 7,10-, 36.4 (37.0); 1,3-, >38.0 (43.3); 6,10-, 47.0 (46.9); 1,6-, 52.3 (53.2); 3.6-, >49.0 (55.1). Fairly good agreement is observed between the experimental and predicted values. More complete analyses of the EPR spectra of the mono-methylated BaP's have been initiated both to confirm the estimated CH_3 splittings (*49*), especially at critical positions in the molecule, and to probe the electronic effects of the methyl substituent on the HOMO. Two methods have been used to confirm the methyl splittings. The first involves computer simulation of the EPR spectra. Usually an unambiguous assignment of the methyl splitting will be forthcoming since there will only be a single group of three equivalent protons which will provide a correct simulation. All the other splittings are expected to be nondegenerate and it would be extremely unlikely for three other protons to have accidently equivalent splittings even under low resolution conditions. The second method involves generation of the radicals in D_2SO_4. It has been shown that rapid H-D exchange occurs at the 1, 3, and 6 positions of BaP on dissolution in D_2SO_4 (*53*). Thus the EPR spectra in D_2SO_4 are changed due to the different nuclear spin of deuterium ($I = 1$), and the considerably reduced splitting constants ($a^D = a^H/6.54$), at these positions. The splitting of the methyl protons should, however, remain unchanged in D_2SO_4, and by examining the EPR spectra one can confirm that the splitting found in H_2SO_4 is also present in D_2SO_4. To date, several of the methylated BaP's have been examined by these two methods. For example, Figure 1 shows the experimental and simulated low resolution EPR spectrum of 7-methyl-BaP. The simulation required a set of four protons with splitting 2.80 gauss; no other sets of three equivalent protons were found, and thus it is assumed that at this resolution the three methyl protons are accidently equivalent to one other proton splitting. This methyl splitting compares favorably with the estimated splitting of 2.65 G and is further confirmed by the presence of the same splitting in the D_2SO_4 spectra. Other methyl splittings which have so far been confirmed by simulation include 9-methyl-BaP (3.57 G compared to estimate of 3.80 G), 10-methyl-BaP (1.15 G compared to estimate of 1.45 G), 3-methyl-BaP (4.56 G compared to estimate of 4.10 G). The remaining methyl splittings have not yet been fully confirmed by spectral simulation of the monomethyl BaP spectra but splittings have been identified in the experimental spectra which are close to the estimated values (see Table

1). Further information is also available from simulations of some of the spectra of the dimethyl-BaP's. Thus, examination of the spectra of 4,5-dimethyl-BaP (*49*) in comparison with the 4- and 5-methyl BaP's indicates that the 4-methyl splitting is ca.0.70 G, as compared to a 5-methyl splitting of 2.20 G. Additionally, the spectra of 1,4-dimethyl-BaP suggests methyl splittings of ca.0.70 G (4-methyl group) and 3.20 G (1-methyl group).

Once the methyl splittings were available for the monomethylated BaP's they could be used as a starting point for the analysis of the unsubstituted BaP cation radical. From high resolution spectra of the wings of the BaP spectrum in H_2SO_4 it was possible to extract potential splitting constants which were confirmed by spectral simulation. Nine splitting constants were found (0.19, 0.37, 0.54, 0.825, 1.94, 2.11, 2.23, 2.85, and 2.95 G) which gave a simulated spectrum of the wings in good agreement with the experimental spectrum (see Fig. 2). To find the three largest splitting constants, a fully deuterated BaP sample was dissolved in H_2SO_4, the deuteriums at positions 1, 3, and 6 are rapidly exchanged for protons (*53*). The spectrum obtained (*50*) is consistent with splittings of 3.77, 4.57, and 6.63 G for these three protons. The assignment of these 12 splittings to the individual positions can be made by comparison to the monomethylated BaP cation radicals. Using the values of the methyl splittings (Table 1), the proton splittings can be assigned in the order of their absolute values. This assumes that methyl substitution does not greatly change the spin density distribution in the molecule. This assumption may not be justified in at least one case, that of the l-methyl-BaP. For various reasons (*50*), the proton splitting in the l-position is assigned as the second-largest proton splitting, in spite of the fact that the l-methyl splitting is only the fifth-largest methyl splitting. The other splittings have been assigned in the same relative order and are as shown in Table 2. From the proton splittings, the absolute values of the spin densities at each position may be calculated using McConnell's equation (see Table 2).

Further justification for these assignments can be obtained from measurements of ^{13}C splittings which were recently made possible with the synthesis of BaPs singly labeled with ^{13}C at each of the 12 protonated carbon atoms (*54,55*). The ^{13}C splitting constants can be obtained by simply measuring the increase in the total width of the EPR spectrum of the ^{13}C derivative over that of the protonated derivative (*50*). Figure 3 shows that under low resolution conditions it is relatively easy to unambiguously locate the outermost lines of the spectra and hence measure the total width. The measured values of each of the 12 protonated positions are shown in Table 2. Theoretically (*56*), the value of the ^{13}C splitting constant depends upon the spin densities at adjacent carbon atoms as well as on the spin density at the carbon atom itself. Using the spin densities calculated from the experimental proton splittings it is possible to calculate the ^{13}C splittings only for positions 2, 8, and 9. Even then complications arise for these positions since the small proton splittings at positions 2 and 8 may correspond to positive or negative spin densities. For positive spin densities, the calculated ^{13}C splittings are -3.45, -2.32, and $^{+}$2.68 G, respectively at positions 2, 8, and 9. For negative spin densities the calculated values are -4.83, -2.79, and 2.87 G. The latter values are clearly in better agreement with the experimental absolute values of 4.55, 2.91 and 3.01 G. For the other nine positions, the ^{13}C splittings were calculated assuming that spin densities at adjacent blind positions (carbons to which no protons are attached) are zero. The best fit was also obtained if the spin density at the 4 position is positive while that at the 11 position is negative (see Table 2), all other positions being positive. Clearly the overall agreement is consistent with the assignments of the proton splittings except, perhaps, for the 5 and 7 positions. Even better agreement can be obtained if the spin densities at the blind positions are appropriately adjusted (see Table 2). These results are sufficiently self consistent to enable reasonable confidence to be placed on the spin densities listed in Table 2 as a reflection of the HOMO of BaP. These values can then be used to test calculational models as well as to rationalize the chemistry and biology of BaP. Table 2 shows the results of a modified Hückel molecular orbital calcula-

Table 1. Summary of EPR data for monomethylated BaP cation radicals.

Methyl substituent	Width of EPR spectra, G	Estimated CH_3 splitting[a]	Experimental CH_3 splitting[b]
None	28.8	—	—
1	35.1	3.15	3.08
2	28.45	<0	0.67
3	37.0	4.1	4.56[b]
4	29.35	0.275	0.26
5	33.9	2.55	2.26[b]
6	44.0	7.6	7.47
7	34.1	2.65	2.80[b]
8	28.8	0	—
9	36.4	3.8	3.57[b]
10	31.7	1.45	1.15[b]
11	30.14	0.68	0.56 or 0.92
12	34.7	2.95	3.43

[a] Estimated CH_3 splitting = (width methyl BaP−width BaP)/2.
[b] Confirmed by simulation.

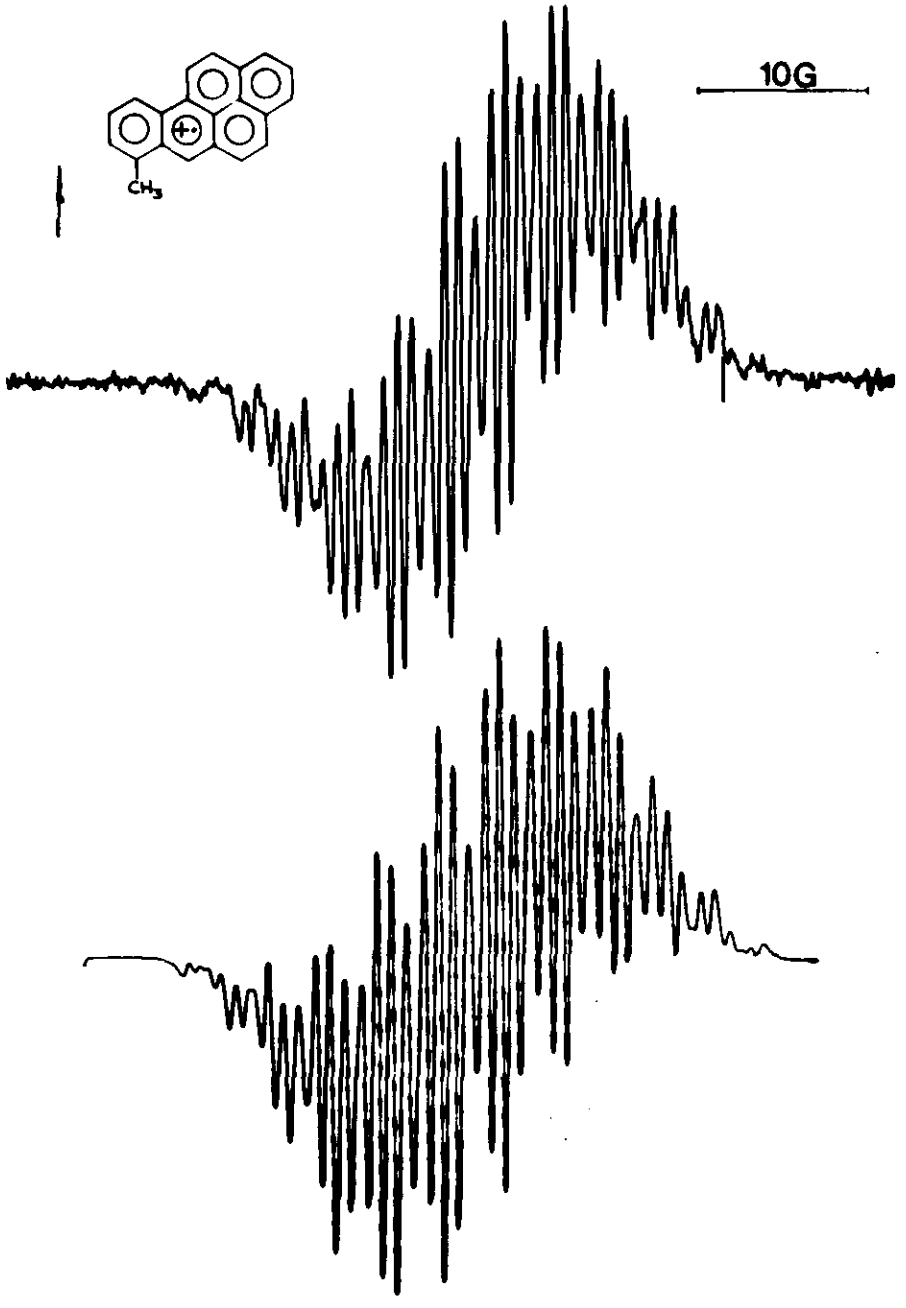

FIGURE 1. Experimental (upper) and simulated (lower) EPR spectra of 7-methyl-BaP in H_2SO_4 (Mod = 0.4 G). Simulation parameters were 1H = 7.14, 1H = 4.45, 2H = 3.62, 4H = 2.80, 1H = 1.92, 1H = 1.18, 1H = 0.66.

tion of the proton splittings. Considering the approximate nature of the calculation the overall agreement with the general features of the experimental values is quite good. Thus, the calculation reproduces the order and magnitude of the largest splittings, 6 > 1 > 3, and indicates that the 2, 8, and 11 positions have the smallest splittings. However, the calculation appears to underestimate the spin density at the 9 and 10 positions while overestimating at the 4 position. Attempts to improve the calculations by varying the overlap integrals do not result in any better agreement nor do more sophisticated calculations (*57,58*). Since the spin densities represent approximately one half of the electron density in the HOMO, and since the latter have been related to the nucleophilic reactivity at the carbon atoms (*57,59*), the observed deviations between the calculated and experimental values could have a significant effect on interpretations or rationalizations of metabolic pathways based on calculated values. For example, the high spin density observed at the 9 position could indicate that direct oxygen insertion to form 9-hydroxy-BaP may account for part or all of the observed metabolic pro-

Table 2. Summary of EPR data for BaP cation radicals.

Position	Methyl splitting in monomethylated BaP cation radical	Assigned proton splittings	Spin densities from proton splittings[a]	^{13}C splittings at each position	Calculated ^{13}C splittings (A)[b]	Calculated ^{13}C splittings (Adjusted)	Calculated proton splittings[c]
1	3.08	4.57	0.163	6.01	6.07	5.92	4.35
2	0.67	0.54	0.0193	4.55	−4.83	−4.83	−1.13
3	4.56	3.77	0.135	4.44	5.07	4.58	3.92
4	0.26	0.37	0.0133	0.93	−0.56	−1.11	2.49
5	2.26	2.11	0.0743	1.32	2.47	1.45	2.40
6	7.47	6.63	0.237	8.30	8.43	8.43	7.37
7	2.80	2.23	0.0793	3.74	2.92	3.93	2.44
8	0.0	0.19	0.0067	2.91	−2.79	−2.79	−0.48
9	3.57	2.95	0.105	3.01	2.87	2.73	1.63
10	1.15	1.94	0.0693	1.29	1.01	1.29	0.40
11	0.92	0.825	0.0294	1.96	−2.39	−1.97	0.40
12	3.43	2.75	0.0971	3.60	3.86	3.71	3.03

[a] Using McConnell's equation $|\rho| = |a|/Q$, $Q = 28$ G.
[b] Assuming negative spin densities at positions 2, 8, and 11.
[c] Calculated using a modified Hückel molecular orbital method.

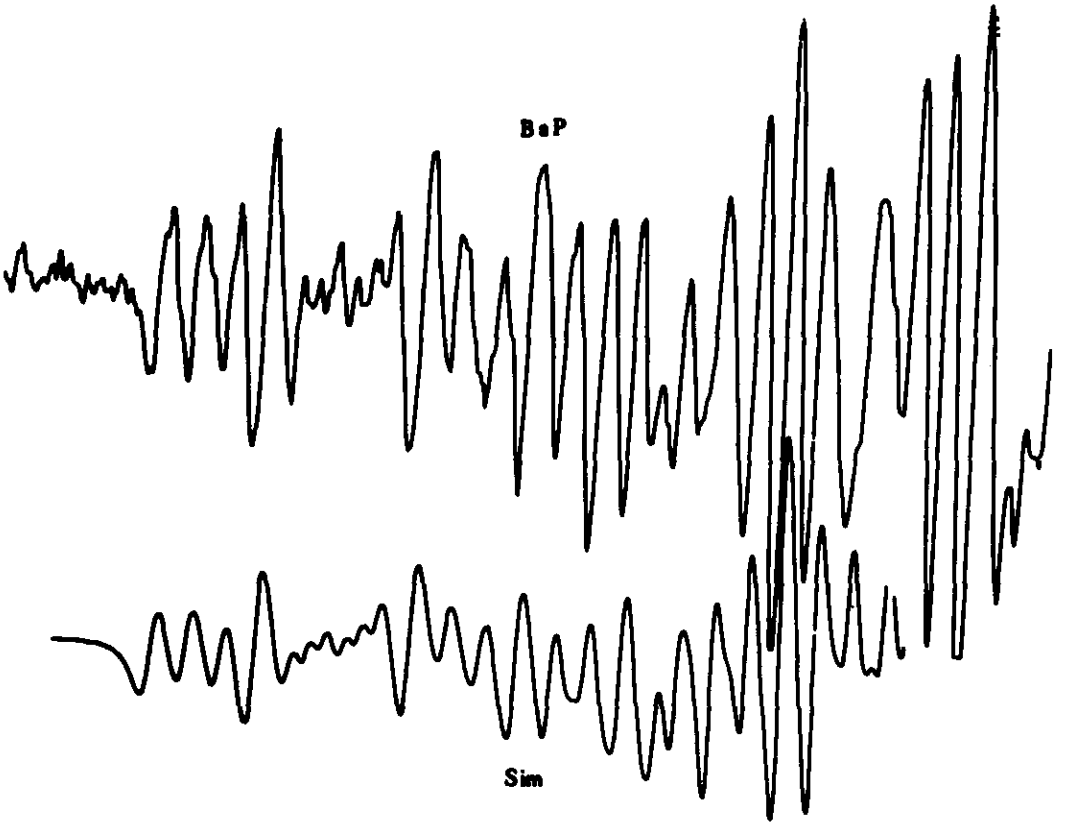

FIGURE 2. Expanded high resolution EPR spectrum (Mod = 0.08 G) of the BaP cation radical in H_2SO_4 (upper trace). Only the low field end of the spectrum is shown. Lower trace is a simulation using 9 inequivalent proton splittings of 0.188, 0.372, 0.541, 0.824, 1.94, 2.11, 2.23, 2.75 and 2.95.

duction of this phenol. Additionally the inequivalence of the 4 and 5 positions is supported by both the results on the methylated BaP's and by the ^{13}C splittings. This inequivalence, which is not reproduced by any method of calculation so far investigated, would explain the selective production of 5-hydroxy-BaP from the isomerization of BaP-4,5-oxide or from the acid dehydration of BaP-4,5-diol (*60*). It is also consistent with the breaking of the C_4-O bond in the enzymatic hydrolysis of BaP-4,5-oxide as observed by Yang et al. (*60*). However, similar selectivity was not observed by Hylarides et al. (*61*) in their study of BaP-4,5-oxide.

Cation Radicals from Hydroxylated and Fluorinated BaPs

Recent experiments in our laboratory with the monohydroxylated BaPs have shown that only 6-and 9-hydroxy-BaP produce stable, well resolved, EPR spectra of their cation radicals when dissolved in H_2SO_4. Several other monohydroxy-BaPs produce observable signals (see Table 3), whereas 12-hydroxy-BaP produces no detectable signal whatsoever. Substitution of a proton by a hydroxyl group is generally expected to reduce the width of a cation radical spectrum, the maximum decrease in width should occur for substitution at the highest spin density positions. The hydroxy-BaP cation radicals whose EPR widths could be measured (Table 3) were in the order 6 < 1 < 3 < 9 < 7 < 5 < 10 < 11, which is consistent with the relative ordering of spin density as determined from the assigned proton splittings in Table 2.

Only the cation radicals from 6-, 7-, 8-, 9- and 10-monofluorinated BaPs produced in sulfuric acid have so far been investigated in our laboratory. On the basis of previous studies with fluorinated naphthalenes (*62*) it is expected that the fluorine splitting constant in a cation radical should be much larger than the proton it is replacing. This is most apparent for the 6-F-BaP$^{\cdot+}$ EPR spectrum which is characterized by a broad doublet of 17.5G in both H_2SO_4 and D_2SO_4. A doublet splitting is also readily observed for 9-F-BaP in D_2SO_4 (~8.2 G) and is just observable for 7-F-BaP in D_2SO_4 (~5 G). The fluorine doublet is not seen for the 8- and 10-F-BaP's in either H_2SO_4 or D_2SO_4. In all cases the fluorine splitting can be estimated from the overall width by subtracting the sum of the proton splittings (see Table 2) at all except the fluorinated position. These estimates are shown in Table 4, together with the calculated fluorine splittings assuming a simple proportionality between the spin density on the adjacent carbon and the fluorine splitting (*62*). The relative ordering of the fluorine splittings, 6 > 9 > 7 > 10 > 8 is in agreement with the previous assignments.

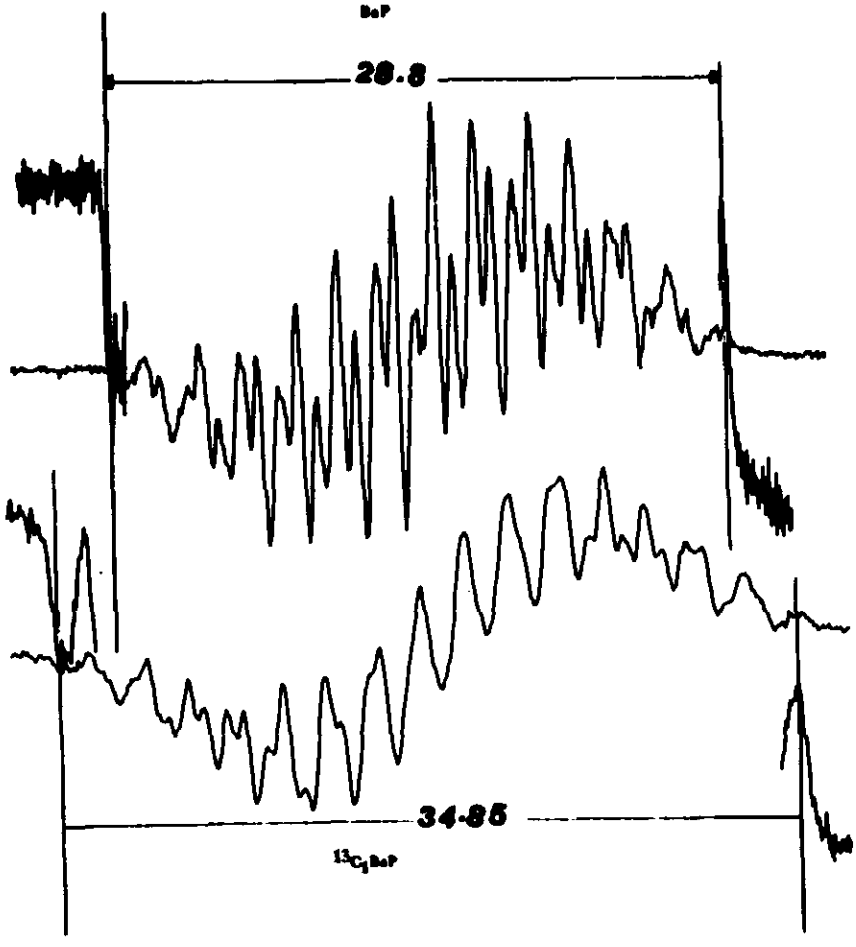

FIGURE 3. The low resolution (Mod = 0.8 G) EPR spectrum of BaP$^{\cdot+}$ (upper) and ^{13}C labeled BaP$^{\cdot+}$ at the 1 position (lower). The insets are the same spectra at higher gain conditions, the measured widths of the unlabeled and labeled BaPs are 28.8 and 34.85 G.

Other EPR Studies of BaP Cation Radicals

A separate EPR study of some 6-substituted BaP cation radicals in H_2SO_4 has given some information on the conformation of the substituent at the 6-position. It is known (*63*) that the splitting of a β-proton is dependent on the dihedral angle θ between the C-H bond axis and the Z axis of the p_Z orbital on the adjacent carbon atom [Eq. (12)]. B_0 is usually small and can be neglected.

$$a_\beta^H = (B_0 + B_2 \cos^2\theta)\, \rho_c^\pi \qquad (12)$$

For a freely rotating methyl group the time-averaged value of $\cos^2\theta$ is 1/2, and therefore, for 6-methyl-BaP, if $a^H{}_\beta = 7.4$ G and $\rho^\pi{}_c = 0.237$, B_2 must equal 62.4 G. If one measures the EPR spectrum of 6-ethyl-BaP in H_2SO_4, one obtains a well resolved signal of width 28.0 G. This spectral width is consistent with a splitting from the two CH_2 protons of the ethyl group of ~2.90 G. This further indicates that the preferred conformation of the ethyl group is one in which the dihedral angle of the CH_2 protons is 60° (Fig. 4*a*). The ratio of β-proton splittings in 6-methyl-and 6-ethyl-BaP, 7.4/2.9 = 2.55 is very similar to the same ratio found (*64*) for hexamethylbenzene and hexaethylbenzene cation radicals, 6.63/2.64 = 2.47, in which the ethyl group adopts a similar preferred conformation. The out of plane position of the CH_3 group probably provides a steric barrier to prevent binding of 6-ethyl-BaP to cytochrome-P-450 and thus accounts for the biological inactivity of this compound.

EPR spectra of 6-hydroxymethyl-BaP and 6-methoxymethyl-BaP in H_2SO_4 and D_2SO_4 are very similar. A poorly resolved signal of width 37–38 G is found in H_2SO_4 and four broad lines which may be due to two large splittings of 13.0 and 6.0 G, are observed in D_2SO_4. These spectra may indicate a preferred conformation for these compounds in which the dihedral angle of the OR group is 30° (Fig. 4*b*). It is also interesting to note that the EPR signal of 6-methyl-BaP in H_2SO_4 changes over a period of one or two hours from one with a width of ~44 G to one with a width of ~37 G. The latter spectrum is very similar to that of the 6-hydroxymethyl-BaP. It seems possible that the first formed 6-methyl-BaP cation radical may react with residual water to produce 6-hydroxymethyl-BaP and its cation radical. As mentioned earlier, BaP also produces a cation radical in the TTFA/TFA system, but the radical has been assigned as a 6-trifluoroacetoxy-BaP cation radical (*10,52*). This trifluoroacetoxylation results in a decrease in the EPR spectral width from 28.8 G in H_2SO_4 to 22.5G in TTFA/TFA. A similar decrease in width is noted with 10-methyl-BaP and 8-F-BaP in TTFA/TFA, suggesting that these compounds are similarly trifluoroacetoxylated at the 6 position. 7-methyl-BaP does not, however, show a decrease in width, indicating that substituents peri to the 6 position can prevent reaction at this position. Similarly, substitution at the 6 position results in the production of the genuine cation radicals from 6-methyl-BaP, 6-ethyl-BaP and 6-methoxy-BaP (*44*). 6-Methyl- and 6-ethyl-BaP give very similar spectra to those obtained in H_2SO_4. However, due to the increased stability of the 6-methyl-BaP radical in TTFA/TFA it has proven possible to obtain an ENDOR spectrum of this radical (P.D. Sullivan and R.C. Sealy, unpublished observations). Comparison of the ENDOR spectrum with the EPR spectrum has provided an analysis in terms of 11 nonequivalent splitting constants, 0.33, 0.43, 0.79, 1.68, 1.89, 2.25, 2.52, 3.07, 3.71, 4.54 and 7.4 (7.4 G is the methyl proton splitting). These values are entirely consistent with those of BaP itself (Table 2) if the smallest splitting is unobservable.

Tkac (*65*) has recently proposed that the EPR signal first observed when a 0.2% solution of BaP in CCl_4 is exposed to oxygen is an ion radical pair resulting from an electron transfer between BaP and O_2 [Eq. (13)].

$$\mathrm{BaP} + \mathrm{O_2} \rightleftarrows \mathrm{BaP^{+}O_2^{-}} \qquad (13)$$

However, the spectrum is not fully resolved, and the parameters given for the BaP cation radical are not in agreement with those proposed in Table 2.

Poorly resolved EPR spectra of the BaP and 6-methyl-BaP cation radicals have also been recently obtained by dissolving the appropriate cation radical salts in TFA or acetonitrile (*36*).

Table 3. Cation radicals from hydroxylated BaPs in H_2SO_4.

Substituted position	Nature of EPR signal	Width of EPR spectrum, G
1	Weak signal, unstable, poor resolution	22.6
2	Weak signal, not resolved, unstable	NM[a]
3	Weak signal, poor resolution	23–24
4	Very weak signal, no resolution	NM[a]
5	Weak, low resolution, unstable	27.2
6	Strong signal, stable, good resolution	21.74
7	Weak signal, low resolution	26.05
8	Very weak signal, no resolution	NM[a]
9	Strong signal, stable, good resolution	25.25
10	Quite strong signal, stable, some resolution	27.43
11	Weak, low resolution	30.0
12	No detectable signal	—

[a] Not measurable.

Table 4. Cation radicals from fluorinated BaPs in H_2SO_4.

Substituted position	Width of EPR spectrum, G	Fluorine splitting estimated from width	Directly observed F splitting	Calculated F splitting[a]
6	~40	17.9	17.5	22.1
7	32–33	6–7	~5	7.4
8	29.8	1.2	—	0.6
9	35–36	10–11	8.2	9.8
10	30.6	3.7	—	6.5

[a] $a_F = Q^F_{Eff}\,\rho_c$, where $Q^F_{Eff} = 93$ G (*62*).

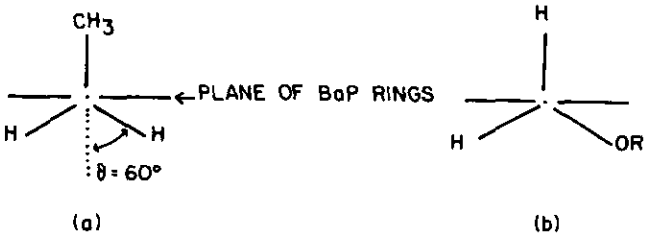

FIGURE 4. Possible conformation of (*a*) 6-ethyl-BaP and (*b*) 6-hydroxy-methyl- or 6-methoxymethyl-BaP.

EPR of Oxygenated BaP Radicals

6-Oxy-BaP

As outlined earlier, the most common radical form of BaP, which is produced both enzymatically and chemically in the presence of oxygen, has been identified as the 6-oxy-BaP radical. Many of the published EPR spectra of this radical are poorly resolved and complete analysis was not possible. The most completely resolved spectrum has been obtained by light irradiation of a BaP solution in CH_2Cl_2 in the presence of a 100% O_2 atmosphere, followed by several freeze-pump-thaw degassing cycles (*10*). This spectrum was analyzed in terms of eleven different splitting constants, as expected for a 6-oxy-BaP radical, with values of 0.11, 0.26, 1.097, 1.102, 1.243, 1.615, 2.591, 2.95, 4.15, 5.15, and 5.65 G. A computer simulation of the spectrum is in excellent agreement with the experimental spectrum. The splitting constants have not been assigned to specific positions although molecular orbital calculations indicate that the 4 largest splittings should be associated with the 1, 3, 4 and 12 protons. More recently, Tkac and Bahna (*65,66*) have suggested a different assignment of the spectra attributed to the 6-oxy-BaP radical. They have argued that such an unhindered phenoxy radical should not be stable in non polar solvents for many weeks, nor should it be unreactive towards hydrogen donating solvents, as is observed. Since the radical is also easily converted to the BaP-3, 6-quinone, (also 1,6- and 6,12-quinones), they have suggested, by analogy with their previous studies on 4,4′-biphenols and 2,2′-biphenols (*67-69*), that the radical may be a paramagnetic radical pair derived from two monoprotonated BaP-3,6-semiquinone radicals (Fig. 5*a,c*). The decrease in EPR signal intensity with temperature is taken as evidence for a shift in the equilibrium between the paramagnetic radical pair (Fig. 5*a,c*) and the diamagnetic quinone-hydroquinone dimer (Fig. 5*b*). The apparent line width alternation which occurs in the EPR spectra under certain conditions is also taken as evidence for rapid exchange of the two hydrogen atoms between the phenoxy and hydroxy groups in positions 3 and 6 (5*a*↔5*c*). There are, however, several arguments which

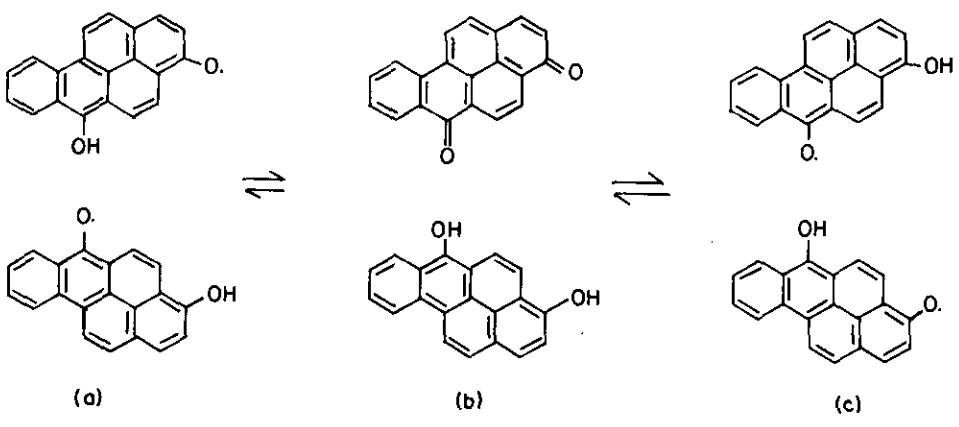

FIGURE 5. Proposed equilibria between paramagnetic radical pair of monoprotonated BaP-3,6-semiquinones (*a*) and (*c*) and diamagnetic quinone-hydroquinone dimer (*b*).

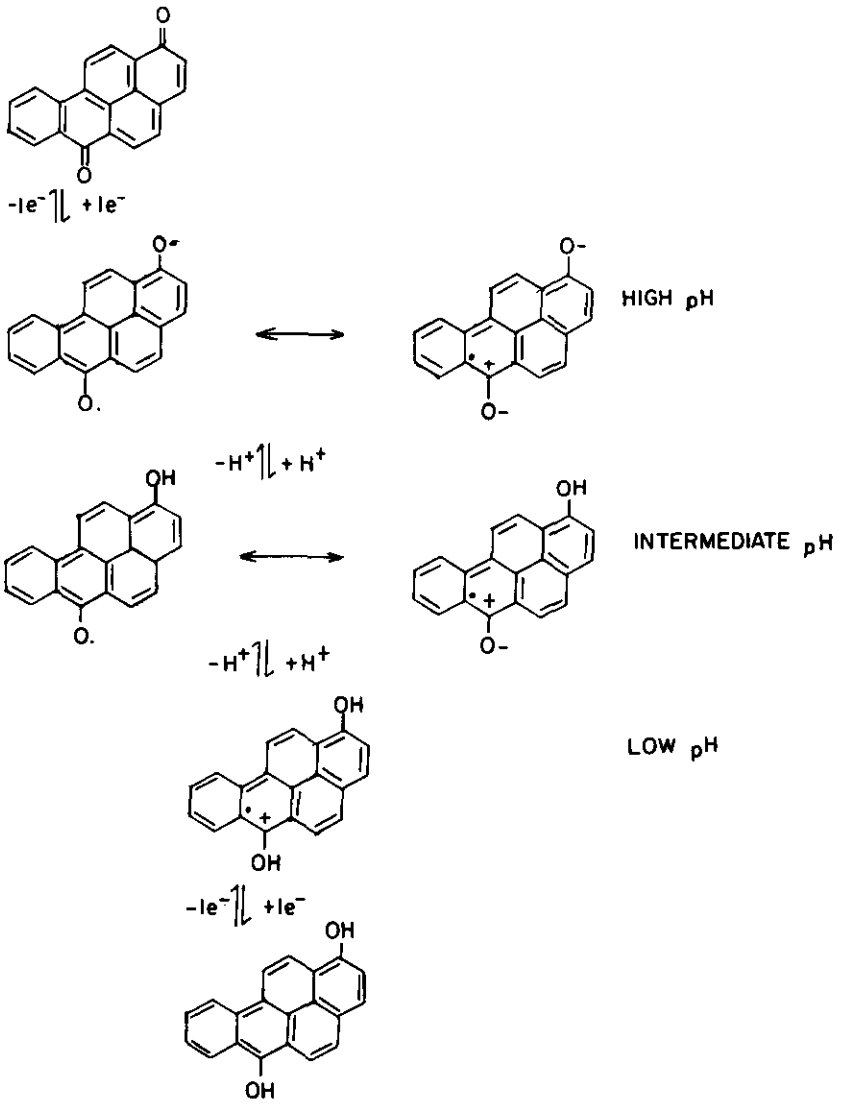

FIGURE 6. Oxidation-reduction of BaP quinones/hydroquinones and structures of intermediate semiquinone anions (high pH), monoprotonated semiquinones (intermediate pH) and diol cations (low pH).

can be made against the proposal of Tkac and Bahna. Substitution of a second oxygen atom at the 3 position should reduce the spectral width considerably below the observed value of ~25 G. The apparent line width alternation phenomena could be an artifact of incomplete resolution. One also might expect, if their interpretation is correct, that the same spectrum should be readily obtained from BaP-3, 6-quinone, whereas in fact the published spectra from this compound are quite different (*3,13*). The unusual stability of the 6-oxy-BaP radical may be due to the fact that a more appropriate representation of this radical is given as an O^- substituted BaP cation radical[Eq. (14), b] rather than a phenoxy radical [Eq. (14), a]. The observed ^{17}O splitting constant of 4.75G (*11*) is also consistent with a much smaller spin density on the oxygen atom than would be expected for a phenoxy radical as is the g value of 2.0032 (*10*).

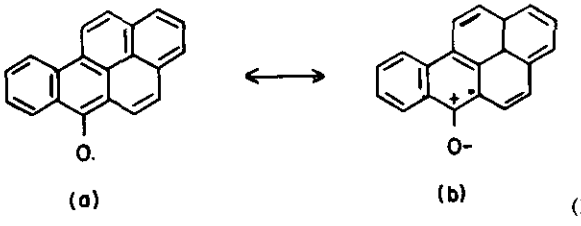

(14)

Overall, the evidence is still in favor of the interpretation of previous workers regarding the assignment of the EPR signal as a 6-oxy-BaP radical.

BaP-Diones

The EPR spectra of the semiquinone radicals obtained by oxidation of the appropriate BaP-diols (1,6-, 3,6- or 6,12-) or by reduction of the BaP-diones have

been observed in solutions of high pH (*3,13*). The spectra are reasonably well resolved and have a width of ~12G, but have not been analyzed in detail. In principle one should be able to observe the mono-protonated semiquinone radicals at intermediate pH and the diprotonated diol cation radicals at very low pH (Fig. 6). These radicals have, however, yet to be observed.

Other Oxy Radicals of BaP

Poorly resolved EPR signals have been observed from several mono-hydroxy substituted BaPs on incubation with rat liver microsomes (*70,71*). 1-, 5-, 7-, 8- and 10-hydroxy BaPs required no NADPH in the incubation mixture to produce an EPR signal, 2-, 4-, 9- and 11-hydroxy BaP only produced a signal when NADPH was included and 3- and 12-hydroxy-BaP did not produce a signal under any conditions.

Oxy Radicals from Substituted BaPs

Substituted BaPs can also produce 6-oxy radicals, under similar chemical or enzymatic conditions as BaP itself, as long as the 6-position is not blocked. Well resolved EPR spectra have been reported for the 6-oxy radicals of 10-methyl-, 7-methyl- and 7,10-dimethyl-BaP in TFA/H_2O_2 (*44*), and unpublished spectra have also been obtained from 7- and 8-F-BaP. None of these spectra have been analyzed in detail.

Reactions of BaP Radicals

Cation Radicals

The reactions of BaP and 6-methyl-BaP cation radicals have been investigated in detail by Cavalieri and co-workers (*17,31,36,72*). They have shown that the BaP cation radical reacts almost exclusively with certain nucleophiles at position 6. 6-Methyl-BaP also reacts with nucleophiles primarily at position 6 with minor contributions from reactions at positions 1 and 3. The BaP cation radical is also quenched by many nitrogenous compounds (*18*) and antioxidants (*73*). Adduct formation with DNA has also been detected via the reaction of BaP cation radicals (*36*).

Electrochemical studies on the cation radicals of mono-methylated BaPs have indicated that their reactions are similar to those of BaP itself (*28*).

Oxy Radicals

As noted earlier, the 6-oxy-BaP radical is unusually stable for a phenoxy radical, being unreactive to many hydrogen-donating solvents (*67,68*) and antioxidant molecules (*73,74*). 6-Hydroxy-BaP binds to DNA and the participation of the 6-oxy-BaP radical in this binding has been suggested by the observed EPR signal when 6-hydroxy-BaP is incubated with the homopolynucleotide poly (G) (*75,76*). The EPR characteristics of the bound complex are, however, somewhat different from the free 6-oxy-BaP radical. The 3,6-BaP-semiquinone radical was also found to bind strongly to poly(G) and DNA with retention of the EPR signal (*76,77*). 1,6-BaP-semiquinone showed a lesser amount of binding and 6,12-BaP-semiquinone did not bind at all. The EPR signals for the 3,6-BaP-semiquinone complex and for the 6-oxy-BaP complex are quite similar and may correspond to the same species.

Other studies have investigated the interaction between the 6-oxy-BaP radical and caffeine, as a model purine base (*78,79*). Using NMR chemical shifts and relaxation times it was concluded that part of the unpaired electron is transferred from 6-oxy-BaP to caffeine and that the most probable structure of the complex has a 6-oxy-BaP molecule sandwiched between two caffeine molecules.

The work reported in this review from our laboratory was supported, in part, by Grant No. CA-34966 awarded by the National Cancer Institute, DHEW.

REFERENCES

1. Robinson, J. Radical anion of benzo(a)pyrene. J. Chem. Phys. 53: 4725–4726 (1970).
2. Kon, H., and Blois, M. S. Paramagnetism of hydrocarbon-conc H_2SO_4 systems. J. Chem. Phys. 38: 743–744 (1958).
3. Nagata, C., Inomata, M., Kodama, M., and Tagashira, Y. Electron spin resonance study of the interaction between the chemical carcinogens and tissue components III. Determination of the structure of the free radical produced either by stirring 3,4-benzopyrene with albumin or incubating it with liver homogenates. Gann 59: 289–298 (1968).
4. Forbes, W. F., Robinson, J. C., and Wright, G. V. Free radicals of biological interest I. Electron spin resonance of tobacco smoke condensates. Can. J. Biochem. 45: 1087–1098 (1967).
5. Elmore, J. J., and Forman, A. EPR of free radical intermediates in oxidation of carcinogenic polycyclic hydrocarbons. Cancer Biochem. Biophys. 1: 115–120 (1975).
6. Forbes, W. F., Robinson, J. C. Possible formation of an azulene-type radical obtained on heating 3,4-benzpyrene. Nature 217: 550–551 (1968).
7. Inomata, M., and Nagata, C. Photoinduced phenoxy radical of 3,4-benzopyrene. Gann 63: 119–130 (1972).
8. Lesko, S., Caspary, W., Lorenzten, R., and Ts'o, P. O. P. Enzymic formation of 6-oxobenzo(a)pyrene radical in rat liver homogenates from carcinogenic benzo(a)pyrene. Biochemistry 14: 3978–3984 (1975).
9. Lorenzten, R. J., Caspary, W. J., Lesko, S. A., and Ts'o, P. O. P. The autoxidation of 6-hydroxybenzo(a)pyrene and 6-oxobenzo(a)pyrene radical, reactive metabolites of benzo(a)pyrene. Biochemistry 14: 3970–3977 (1975).
10. Menger, E. M., Spokane, R. B., and Sullivan, P. D. Free radicals derived from benzo(a)pyrene. Biochem. Biophys. Res. Communs. 71: 610–616 (1976).
11. Rispin, A. S., Kon, H., and Nebert, D. W. Electron spin resonance study of ^{17}O-enriched oxybenzo(a)pyrene radical. Mol. Pharmacol. 12: 476–482 (1976).
12. Ioki, Y., and Nagata, C. A fluorimetric and esr study of the oxygenation of benzo(a)pyrene; an interpretation of the enzymic oxygenation. J. Chem. Soc. Perkin II: 1172–1175 (1977).
13. Lorenzten, R. J., and Ts'o, P. O. P. Benzo(a)pyrenedione/benzo(a)pyrenediol oxidation-reduction couples and the generation of reactive reduced molecular oxygen. Biochemistry 16: 1467–1474 (1977).
14. Wilk, M., Bez, W., and Rochlitz, J. Neue Reaktionen der carcinogenen Kohlenwasserstoffe 3,4-Benzpyren, 9,10-Dimethyl-1,2-benzanthracen und 20-Methylcholanthren. Tetrahedron 22: 2599–2608 (1966).

15. Fried, J., and Schumm, D. E. One electron transfer oxidation of 7,12-dimethyl-benzo(a)anthracene, a model for the metabolic activation of carcinogenic hydrocarbons. J. Am. Chem. Soc. 89: 5508–5509 (1967).
16. Fried, J. One electron oxidation of polycyclic aromatics as a model for the metabolic activation of carcinogenic hydrocarbons. In: Chemical Carcinogenesis Part A (P. O. P. Ts'o and J. DiPaolo, Eds.), M. Dekker, New York, 1974, pp. 197–215.
17. Cavalieri, E., and Auerbach, R. Reactions between activated benzo(a)pyrene and nucleophilic compounds, with possible implications on the mechanism of tumor initiation. J. Natl. Cancer Inst. 53: 393–397 (1974).
18. Caspary, W., Cohen, B., Lesko, S., and Ts'o, P. O. P. Electron paramagnetic resonance study of iodine induced radicals of benzo(a)pyrene and other polycyclic hydrocarbons. Biochemistry 12: 2649–2656 (1969).
19. Goez-Morales, G., and Sullivan, P. D. Electron paramagnetic resonance studies of ion pairs in solutions of cation radicals. J. Am. Chem. Soc. 96: 7232–7237 (1974).
20. Schlesener, C. J., Amatore, C., and Kochi, J. K. Kinetics and mechanism of aromatic oxidative substitutions via electron transfer. Applications of Marcus theory to organic processes in the endergonic region. J. Am. Chem. Soc. 106: 3567–3577 (1984).
21. Rochlitz, J. Neue Reaktionen der carcinogenen Kohlenwasserstoffe-II. Tetrahedron 23: 3043–3048 (1967).
22. Wilk, M., and Girke, W. Reactions between benzo(a)pyrene and nucleolases by one electron oxidation. J. Natl. Cancer Inst. 49: 1585–1597 (1972).
23. Jeftic, L., and Adams, R. N. Electrochemical oxidation pathways of benzo(a)pyrene. J. Am. Chem. Soc. 92: 1332–1337 (1970).
24. Blackburn, G. M., Taussig, P. E., and Will, J. P. Binding of benzo(a)pyrene to DNA investigated by tritium displacement. J. Chem. Soc. Chem. Commun. 1974: 907–908 (1974).
25. Lesko, S. A., Ts'o, P. O. P., and Umans, R. S. Interaction of nucleic acids V. Chemical linkage of 3,4-benzpyrene to deoxyribonucleic acid in aqueous solution. Biochemistry 8: 2291–2298 (1973).
26. Hoffman, H. D., Lesko, S. A., and Ts'o, P. O. P. Chemical linkage of polycyclic hydrocarbons to deoxyribonucleic acids and polynucleotides in aqueous solution and in a buffer-ethanol solvent system. Biochemistry 9: 2594–2604 (1970).
27. Rogan, E., Roth, R., Katomski, P., Benderson, J., and Cavalieri, E. Binding of benzo(a)pyrene at the 1,3,6 positions to nucleic acids *in vivo* on mouse skin and *in vitro* with rat liver microsomes and nuclei. Chem.-Biol. Interact, 22: 35–51 (1978).
28. Tryk, D. A., Park, S.-M., and Daub, G. H. Electrochemical determination of cation radical stabilities of monomethylbenzo(a)pyrenes. J. Electrochem. Soc. 130: 597–603 (1983).
29. Sullivan, P. D. EPR Studies of methylated benzo(a)pyrene cation radicals. J. Magnetic Res. 54: 314–318 (1983).
30. Cavalieri, E. L., Rogan, E. G., Roth, R. W., Saugier, R. K., and Hakam, A. The relationship between ionization potential and horseradish peroxidase/hydrogen peroxide catalyzed binding of aromatic hydrocarbons to DNA Chem. Biol. Interact. 47: 87–109 (1983).
31. Rogan, E., Roth, R., and Cavalieri, E. Manganic acetate and horseradish peroxidase/hydrogen peroxide: *in vitro* models of activation of aromatic hydrocarbons by one electron oxidation. In: Polynuclear Aromatic Hydrocarbons: Chemistry and Biological Effects (A. Bjorseth and A. J. Dennis, Eds.), Battelle Press, Columbus, Ohio, 1980, pp. 259–266.
32. Cavalieri, E., Roth, R., and Rogan, E. G. Metabolic activation of aromatic hydrocarbons by one-electron oxidation in relation to the mechanism of tumor initiation. In: Carcinogenesis, Vol. 1. Polynuclear Aromatic Hydrocarbons: Chemistry, Metabolism, and Carcinogenesis (R. I. Freudenthal and P. W. Jones, Eds.), Raven Press, New York, 1976, pp. 181–190.
33. Tay, L. K., Sydnor, K. L., and Flesher, J. W. Binding of 6-hydroxymethylbenzo(a)pyrene and 6-acetoxymethylbenzo(a)pyrene to DNA. Chem. Biol. Interact. 25: 35–44 (1979).
34. Cavalieri, E., Roth, R., and Rogan, E. Hydroxylation and conjugation at the benzylic carbon atom: a possible mechanism of carcinogenic activation for some methyl-substituted aromatic hydrocarbons. In: Polynuclear Aromatic Hydrocarbons (P. W. Jones and P. Leber, Eds.), Ann Arbor Science, Ann Arbor, MI, 1979, pp. 517–529.
35. Rogan, E. G., Hakam, A., and Cavalieri, E. Structure elucidation of a 6-methylbenzo(a)pyrene-DNA adduct formed by horseradish peroxidase *in vitro* and mouse skin *in vivo*. Chem. Biol. Interact. 47: 111–122 (1983).
36. Cavalieri, E., Rogan, E., Warner, C., and Bobst, A. Synthesis and characterization of benzo(a)pyrene and 6-methylbenzo(a)pyrene radical cations. In: Polynuclear Aromatic Hydrocarbons: Mechanisms, Materials, and Metabolism (M. Cooke and A. J. Dennis, Eds.),Battelle Press, Columbus, Ohio, 1985, pp. 227–236.
37. Selkirk, J. K. Comparison of epoxide and free-radical mechanisms for activation of benzo(a)pyrene by Sprague-Dawley rat liver microsomes. J. Natl. Cancer Inst. 64: 771–774 (1980).
38. Capdevila, J., Estabrook, R. W., and Prough, R. A. Differences in the mechanism of NADPH and cumene hydroperoxide supported reactions of cytochrome P-450. Arch. Biochem. Biophys. 200: 186–195 (1980).
39. Yang, S. K., Deutsch, J., and Gelboin, H. V. Benzo(a)pyrene metabolism: activation and detoxification. In: Polycyclic Hydrocarbons and Cancer 1. Environment, Chemistry and Metabolism (H. V. Gelboin and P. O. P Ts'o, Eds). Academic Press, New York, 1978, pp. 205–224.
40. Jerina, D. M., Yagi, H., Lehr, R. E., Thakker, D. R., Schaefer-Ridder, M., Karle, J. M., Levin, W., Wood, A. W., Chang, R. L., and Conney, A. H. The Bay-region theory of carcinogenesis by polycyclic aromatic hydrocarbons. In: Polycyclic Hydrocarbons and Cancer. 1. Environment, Chemistry and Metabolism (H. V. Gelboin and P. O. P. Ts'o, Eds.), Academic Press, New York, 1978, pp. 173–188.
41. Wood, A. W., Levin, W., Chang, R. L., Yagi, H., Thakker, D. R., Lehr, R. E., Jerina, D. M., and Conney, A. H. Bay-region activation of carcinogenic polycyclic hydrocarbons. In: Polynuclear Aromatic Hydrocarbons (P. W. Jones and P. Leber, Eds.), Ann Arbor Science, Ann Arbor, MI, 1979, pp. 531–551.
42. Nagata, C., Tagashira, Y., and Kodama, M. Metabolic activation of benzo(a)pyrene: significance of the free radical. In: Chemical Carcinogenesis, Part A (P. O. P. Ts'o and J. A. DiPaolo, Eds.) Marcel Dekker, New York, 1974, pp. 87–111.
43. Ts'o, P. O. P., Caspary, W. J., and Lorentzen, R. J. The involvement of free radicals in chemical carcinogenesis. In: Free Radicals in Biology. Vol. III (W. A. Pryor, Ed.), Academic Press, New York, 1977, pp. 251–303.
44. Sullivan, P. D., Ellis, L. E., Calle, L. M., and Ocasio, I. J. Chemical and enzymatic oxidation of alkylated benzo(a)pyrenes. Chem.-Biol. Interact. 40: 177–191 (1982).
45. Seybold, P. G. and Graslund, A. A molecular orbital study of the metabolism and carcinogenicity of the phenols of benzo(a)pyrene. Int. J. Quantum Chem: Quantum Biol. Symp. 7: 261–270 (1980).
46. Seybold, P. G. Aryloxy radical formation as a deactivating process in chemical carcinogenesis: phenolic derivatives of 7,12-dimethylbenz(a)anthracene and 5-methylchrysene. Int. J. Quantum Chem: Quantum Biol. Symp. 7: 271–276 (1980).
47. Levin, W., Wood, A. W., Wislocki, P. G., Chang, R. L., Kapitulnik, J., Mah, H. D., Yagi, H., Jerina, D. M., and Conney, A. H. Mutagenicity and carcinogenicity of benzo(a)pyrene and benzo(a)pyrene derivatives. In: Polycyclic Hydrocarbons and Cancer, Vol. 1 (H. V. Gelboin and P. O. P. Ts'o, Eds.) Academic Press, New York, 1978, pp. 189–202.
48. Pryor, W. A. Mechanisms and detection of pathology caused by free radicals. Tobacco smoke, nitrogen dioxide and ozone. In: Environmental Health Chemistry—Chemistry of Environmental Agents as Potential Human Hazards (J. D. MCKinney, Ed.), Ann Arbor Science, Ann Arbor, MI, 1980, pp. 445–465.
49. Sullivan, P. D., Bannoura, F., and Roach, S. Cation radicals of methylated benzo(a)pyrenes. In: Polynuclear Aromatic Hydrocarbons: Mechanisms, Methods and Metabolism (M. Cooke and A. J. Dennis, Eds.), Battelle Press, Columbus, OH, 1985, pp. 1273–1283.
50. Sullivan, P. D., Bannoura, F., and Daub, G. H. ^{13}C and ^{1}H EPR analysis of the benzo(a)pyrene cation radical. J. Am. Chem. Soc. 107: 32–35 (1985).
51. Sullivan, P. D., Calle, L. M., Ocasio, I. J., Kittle, J. D., and

Ellis, L. E. The effects of antioxidants on the mutagenicity of benzo(a)pyrene and derivatives. In: Polynuclear Hydrocarbons: Chemistry and Biological Effects, (A. Bjorseth and A. J. Dennis, Eds.) Battelle Press, Columbus, Ohio, 1980, pp. 163–175.

52. Sullivan, P. D., Menger, E. M., Reddoch, A. H., and Paskovich, D. H. Oxidation of anthracene by thallium (III) trifluoroacetate. Electron spin resonance and structure of the product cation radicals. J. Phys. Chem. 82: 1158–1160 (1978).
53. Cavalieri, E., and Calvin, M. 220 MHz nuclear magnetic resonance analysis and selective deuterio-deprotonation of benzo(a)pyrene and 6-methylbenzo(a)pyrene. J. Chem. Soc. Perkin Trans 1: 1253–1256 (1972).
54. Bodine, R. S., Hylarides, M. D., Daub, G. H., VanderJagt, D. L. ^{13}C-Labeled benzo(a)pyrene and derivatives. I. Efficient pathways to labeling the 4,5,11 and 12 positions. J. Org. Chem. 43: 4025–4028 (1978).
55. Unkefer, C. J., London, R. E., Whaley, T. W., and Daub, G. H. ^{13}C and ^{1}H NMR Analysis of isotopically labeled benzo(a)pyrenes. J. Am. Chem. Soc. 105: 733–735 (1983).
56. Karplus, M., and Fraenkel, G. K. Theoretical interpretation of carbon-13 hyperfine interactions in electron spin resonance spectra. J. Chem. Phys. 35: 1312–1323 (1961).
57. Loew, G. H., Wong, J., Phillips, J., Hjelmeland, L., and Pack, G. Quantum chemical studies of the metabolism of benzo(a)pyrene. Cancer. Biochem. Biophys. 2: 123–130 (1978).
58. Shipman, L. L. Ab initio quantum mechanical characterization of the ground electronic state of benzo(a)pyrene. Implications for the mechanism of polynuclear aromatic hydrocarbon oxidation to epoxides by cytochrome P-450. In: Carcinogenesis, Vol. 3: Polynuclear Aromatic Hydrocarbons (P. W. Jones and R. I. Freudenthal, Eds.), Raven Press, New York, 1978, pp. 139–144.
59. Fu, P. P., Harvey, R. G., and Beland, F. A. Molecular orbital theoretical prediction of the isomeric products formed from reactions of arene oxides and related metabolites of polycyclic aromatic hydrocarbons. Tetrahedron 34: 857–866 (1978).
60. Yang, S. K., Roller, P. P., and Gelboin, H. V. Enzymatic mechanism of benzo(a)pyrene conversion to phenols and diols and an improved hplc separation of benzo(a)pyrene derivatives. Biochemistry 16: 3680–3687 (1977).
61. Hylarides, M. D., Lyle, T. A., Daub, G. H., and VanderJagt, D. L. Carbon-13 nmr study of nucleophilic additions to benzo(a)pyrene 4,5-oxide and of its acid catalyzed rearrangement. J. Org. Chem. 44: 4652–4657 (1979).
62. Thomson, C., and MacCulloch, W. J. ESR spectra of the cation radicals of some highly fluorinated naphthalenes. Mol. Phys. 19: 817–832 (1970).
63. Heller, C., and McConnell, H. M. Radiation damage in organic crystals II. Electron spin resonance of (CO_2H) $CH_2CH(CO_2H)$ in β-succinic acid. J. Chem. Phys. 32: 1535–1539 (1960).
64. Carter, M. K., and Vincow, G. Electron spin resonance of the hexamethylbenzene and hexaethylbenzene positive-ion radicals. J. Chem. Phys. 47: 302–312 (1967).
65. Tkac, A., and Bahna, L. Reactivity of free and coordinated radicals in biology and chemical carcinogenesis II. Electron transfer from 3,4-benzopyrene to molecular oxygen and to peroxides, and interpretation of ESR signals of the intermediate radicals of oxidation. Neoplasma 30: 197–232 (1983).
66. Tkac, A., and Bahna, L. Reactivity of free and coordinated radicals in biology and chemical carcinogenesis I. Coordinated phenoxy radicals generated by hydrogen transfer from hydroxy derivatives of 3,4-benzopyrene. Neoplasma 29: 497–516 (1982).
67. Pelikan, P., Tkac, A., Omelka, L., and Stasko, A. Radical reactions in the coordination sphere of transition metals. XIV. Spin distribution of phenoxy radicals generated from biphenyldiols. Org. Magn. Resonance 20: 205–211 (1982).
68. Tkac, A., Omelka, L., Jirackova, L., and Pospisil, J. Radical reactions in the coordination sphere of transition metals. IX. Phenoxy and cyclohexadienonyloxy radicals derived from 2,2′-biphenyldiols and 2,2′-thiobisphenols. Org. Magn. Resonance 14: 171–176 (1980).
69. Tkac, A., Omelka, L., Jirackova, L., and Pospisil, J. Radical reactions in the coordination sphere of transition metals. X. Radicals derived from 4,4′-biphenyldiols, 4,4′-thiobisphenols and bis-(4-hydroxybenzyl) sulfide. Org. Magn. Resonance 14: 249–255 (1980).
70. Kimura, T., Kodama, M., and Nagata, C. Electron spin resonance study on the metabolism of twelve mono-hydroxy benzo(a)pyrenes in liver microsomes. Gann 71: 417–418 (1980).
71. Caspary, W. J., Carroll, C., Morton, R., Dinces, N., Ts'o, P. O. P., and Harvey, R. G. Metabolism of 1-hydroxybenzo(a)pyrene. Chem.-Biol. Interact. 36: 311–317 (1981).
72. Cavalieri, E., and Rogan, E. One electron oxidation of aromatic hydrocarbons in chemical and biological systems. In: Polynuclear Aromatic Hydrocarbons: Formation, Metabolism and Measurement (M. Cooke and A. J. Dennis, Eds.), Battelle Press, Columbus, Ohio, 1980, pp. 1–26.
73. Sullivan, P. D., Calle, L. M., Shafer, K., and Nettleman, M. Effect of antioxidants on benzo(a)pyrene free radicals. In: Carcinogenesis, Vol. 3. Polynuclear Aromatic Hydrocarbons (P. W. Jones and R. I. Freudenthal, Eds.) Raven Press, New York, 1978, pp. 1–8.
74. Krzywanska, E., and Piekarski, L., Benzo(a)pyrene free radicals formation in the presence of butylated hydroxyanisole and their possible importance in carcinogenesis. Neoplasma 24: 395–400 (1977).
75. Kodama, M., and Nagata, C. Binding of 6-oxybenzo(a)pyrene radical with DNA and polynucleotides. Gann 68: 125–126 (1967).
76. Nagata, C., Kodama, M., and Ioki, Y. Electron Spin Resonance Study of the binding of the 6-oxybenzo(a)pyrene radical and benzo(a)pyrenesemiquinone radicals with DNA and polynucleotides. In: Polycyclic Hydrocarbons and Cancer. Vol. 1. Environment, Chemistry and Metabolism (H. V. Gelboin and P. O. P. Ts'o, Eds.), Academic Press, New York, 1978, pp. 247–260.
77. Kodama, M., Ioki, Y., and Nagata, C. Binding of benzo(a)pyrene-semiquinone radicals with DNA and polynucleotides. Gann 68: 253–254 (1977).
78. Mishra, K. P., Nosaka, Y., Akasaka, K., Nagata, C., and Hatano, H. Solubilization of 6-oxybenzo(a)pyrene radical by caffeine and DNA as studied by magnetic resonance. Observation of intermolecular charge transfer. Biochim. Biophys. Acta 520: 679–687 (1978).
79. Nosaka, Y., Akasaka, K., and Hatano, H. Interaction of benzo(a)pyrene and 6-oxybenzo(a)pyrene with caffeine. Structure of the complexes as studied by NMR chemical shift and relaxation. J. Phys. Chem. 82: 2829–2833 (1978).